*34th EPS Conference on Plasma Phys. Warsaw, 2 - 6 July 2007 ECA Vol.**31F**, P-2.052 (2007)*

The effect of EC heating on impurity transport in T-10

N.Timchenko, V.Vershkov, V.Karakcheev, D.Shelukhin, A.Dnestrovskij,V.Krupin, A.Gorshkov, D.Ryzhakov, I.Bel'bas

Institute of Nuclear Fusion, RRC "Kurchatov Institute", Moscow, Russia

Results from different devices have shown that impurity accumulation can be reduced by central EC heating [1]. On T-10 the experiments with the central ECH have shown the reduction of the central impurity density as well. To control impurities behavior the understanding of the underlined transport and study of parametric dependences is of importance. In on-axis ECH discharges impurity expulsion from the plasma center is mainly related to an increase in the central anomalous transport. To investigate the effect of EC heating on impurity behavior and understand the role of ECH radial location the experiments on T-10 in both on- and off-axis ECH regimes have been carried out. Application of off-axis ECH enables to suppress sawtooth oscillations as well.

EXPERIMENTAL SETUP AND DATA ANALYSIS

To analyze the effect of EC heating on impurity transport a short argon gas-puff (t~15-20 ms) was applied in a stationary phase of both OH and ECH discharges. The argon density profile evolution after puffing was studied by measurements of the He- and H-like argon ions line radiation. The registration of radiation of 2p – 1s Ar^{+16} and Ar^{+17} lines was carried out by means of the X-ray crystal monochromator RM-2 with multiwire gas chamber which enables to register 48 chords with time resolution of 10 μs. The measurements were made for both argon lines emission and recombination continuum radiation in a series consisting of reproducible discharges by means of wavelength change in the crystal monochromator from pulse to pulse.

Two types of ohmic heating discharges and corresponding to them two types of ECH discharges, characterized by different EC power space deposition, are compared. Working parameters are as follows: the plasma current I_p = 250 kA, the central line averaged density $n_e = 2.5\times10^{19}$ m^{-3} and the EC power 0.75 - 1 MW in the case of the centrally deposited ECH; I_p = 180 kA, $n_e = 1.5\times10^{19}$ m^{-3}, the EC power of 650 MW for off-axis EC heating placed at ρ~0.4. Sawtooth activity was suppressed in the regimes with off-axis EC heating, in other discharges of this series, sawteeth were presented. Argon gas-puff has been performed in all four types of OH and EC regimes for transport study. The argon density evolution at the transition from OH to ECH regime was analyzed as well.

For impurity transport simulations two impurity transport codes, T-10 impurity code [2] and STRAHL code have been used. The main plasma simulations were carried out by means of ASTRA code [3]. Impurity transport analysis is based on solutions of the radial transport equations together with ionization balance for all ionization stages of argon

$$\frac{\partial n_i^Z}{\partial t} = \frac{1}{r}\frac{\partial}{\partial r} r\left(D(r)\frac{\partial n_i^Z}{\partial r} - V(r) n_i^Z \right) + S_{i-1} n_{i-1}^Z - S_i n_i^Z + R_{i+1} n_{i+1}^Z - R_i n_i^Z$$

where $D(r)$ and $V(r)$ are the flux surface averaged diffusion coefficient and convection velocity respectively, $S_i(T_e,Z_i)$, $R_i(T_e,Z_i)$ are ionization and recombination rates including the charge-exchange recombination for a specific ion with the charge Z_i correspondently.

EXPERIMENTAL RESULTS AND SIMULATIONS

In Fig.1a and Fig.1b the experimental data on the central argon density and the central electron density reduction in ECH plasma compared to OH regime for on- and off-axis ECH are shown. The data are presented versus total input power.

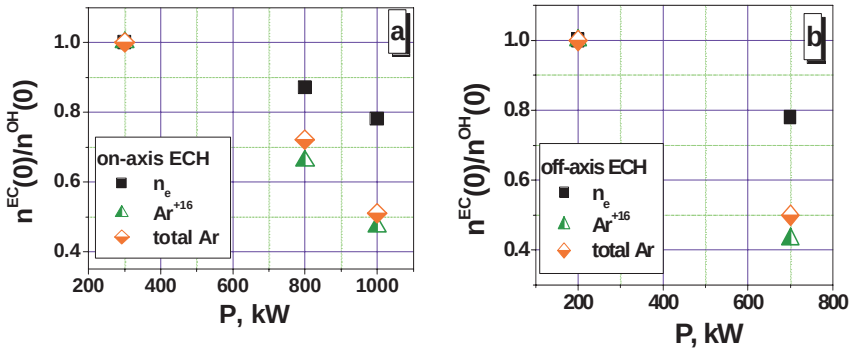

Fig.1(a). *The decrease of the central argon density and electron density in ECH plasma compared to OH regime versus total power* (a) in *on-axis ECH (b)* in *off-axis ECH.*

Fig.1a shows that in the central ECH plasma both Ar and electron density expulsion is proportional to the total input power. Comparison of the results presented in Fig.1a and Fig.1b shows that there is only a minor change in central Ar and electron densities decrease between the different heating scenarios taking into account approximately the same relative power increase compared to OH regimes in both heating schemes. To analyze the impurity behavior transport calculations in on- and off-axis ECH have been performed. Spectroscopic data used

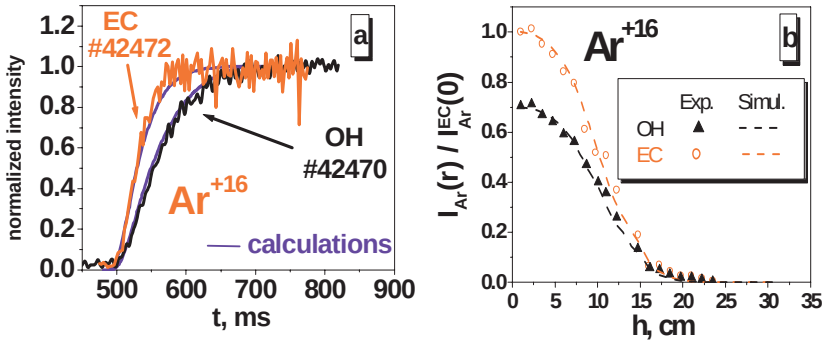

Fig.2 *(a)the time evolution and (b) the steady-state profiles of chord line radiation in OH and on-axis ECH regime. Experiment and simulation.*

for transport calculations are given in Fig.2. (a) and (b). Fig.2a shows evolution of the central chord line radiation in OH and on-axis ECH regimes after Ar puffing. Ar^{+16} chord radiation profiles in steady-state are shown in Fig.2b.

The transport coefficients presented in Fig.3a reveal that in both on- and off-axis ECH

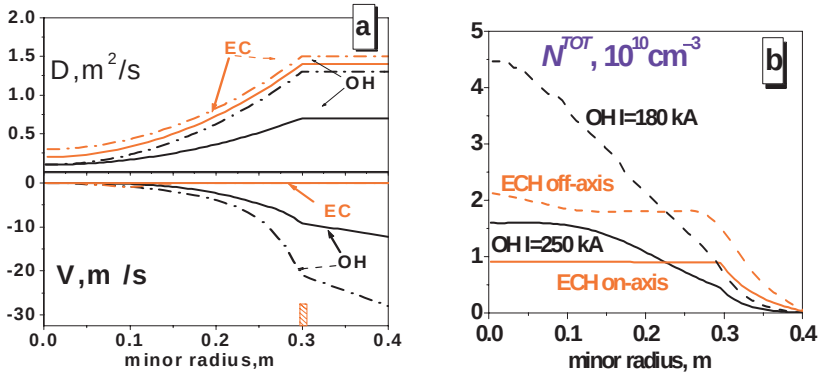

Fig.3 *(a)The transport coefficients in OH and ECH regime, (b)The total Ar density profiles in OH and ECH regimes.*
The solid curves refer to OH plasma with I=250 kA and on-axis ECH(#42472), the dash curves refer to OH plasma with I=180kA and off-axis ECH(#44271) .

plasmas argon transport is strongly modified compared to OH regimes. In the case of the central EC heating the diffusion coefficients increase approximately by a factor of two whereas the pinch velocity reduces up to the negligible values. Simulated total argon density profiles in OH and EC regimes are drawn in Fig.3b. In the central ECH discharge the Ar density profile is flat with the central argon concentration decreased compared to OH plasma. In the OH regime of the second type (I=180 kA) both the electron and the impurity density profiles are more peaked than in the OH regime of the fist type (I=250 kA). In the presence of off-axis deposited ECH the diffusion coefficients increase and the inward pinch is suppressed as well as in the case of the central EC heating. Fig.3b show that off-axis ECH flattens the argon density profile with argon concentration decrease in the plasma center as well. An increase of diffusion in the plasma center in off-axis ECH is supported by turbulence reflectometry measurements which show that the level of the central density perturbations rises by a factor of two in off-axis ECH compared to OH regime [4].

Transport coefficients simulated in both OH and EC plasmas were used for modeling of argon density evolution after ECH application. Measured time traces of the main parameters in the case of off-axis ECH are shown in Fig.4. Argon ions density evolution shown in Fig.5 and evolution of the ratio of the total Ar density to the electron density $n^{Ar}(0)/ n_e(0)$ in Fig.6 demonstrates argon expulsion and greater argon density decrease compared to the electron density decrease in ECH plasma compared to OH regime.

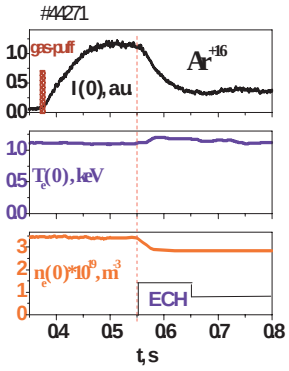

Fig.4. Measured time traces of Ar^{+16} chord line radiation, n_e, T_e

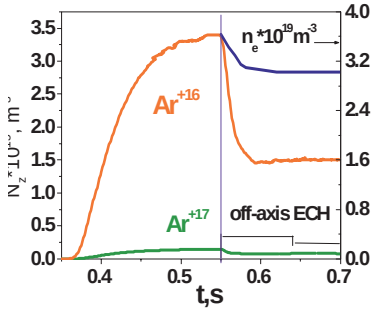

Fig.5.Simulated Ar ions and electron densities evolution in OH regime and after off-axis ECH switch on.

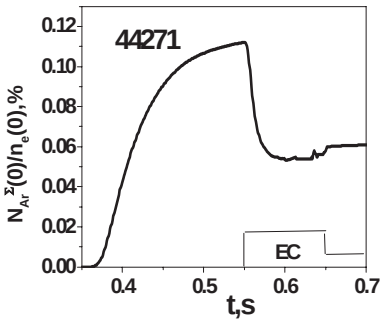

Fig.6. Simulated total argon density expulsion from the plasma center

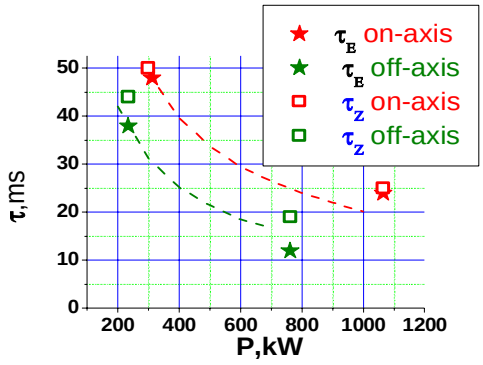

Fig.7 Energy confinement times and impurity confinement times (decay times) versus the total power. ---- ITER scaling L- mode $\tau_E \sim 1/P^{0.73}$

Impurity confinement times obtained from the experimental data (decay times for pellet-injection or the rate of approaching the steady-state after short gas puff) are placed in Fig.7 versus total power. Energy confinement times are presented as well. It is seen that in both OH and ECH regimes energy and impurity confinement times decrease with an increase of total input power.

CONCLUSIONS

In on-axis EC heating regimes argon density is found to decrease in the plasma center, the argon density reduction being proportional to the total input power. At the same time the central electron density decreases approximately in a factor of two smaller than the impurity density.

In the off-axis ECH regimes the central argon density expulsion is found to be approximately the same as in on-axis ECH regimes. The increase of the central impurity transport in off-axis ECH plasma is supported by the turbulence level increase compared to OH regime. The simulations have shown that the effect of ECH on impurity transport both in on-axis and off-axis ECH plasma is related to the increase in anomalous diffusivity and inward pinch suppression. In T-10 the impurity confinement times for both OH and ECH regimes are close to the energy confinement times and reduce with the total input power increase.

The authors are grateful to Dr. R. Dux for opportunity of using the code STRAHL.

The work was carried out by financial support of the Nuclear Science and Technology department of RosAtom RF, Scientific School GK 02.516.11.6068, INTAS1000008-8046 and NOW-RFBR Grant 047. 016.015.

REFERENCES

1. R. Dux et al., Plasma Phys. Control.Fusion, 45(2003)1815
2. Yu.N. Dnestrovskij., V.F. Strizhov. Model of impurity diffusion in tokamaks. Preprint IAE 3779, M., 1983
3. G.V. Pereverzev, P.N. Yushmanov. ASTRA Automated System for Transport Analysis in a Tokamak. IPP report 5/98 (2002).
4. V. Vershkov et al., Nucl. Fusion, 45 (2005) S203